

Characterization of the Redox Activity and Disulfide Bond Formation in Apurinic/Apyrimidinic Endonuclease

Meihua Luo,[†] Jun Zhang,[§] Hongzhen He,[‡] Dian Su,[§] Qiuja Chen,[‡] Michael L. Gross,[§] Mark R. Kelley,^{*,†} and Millie M. Georgiadis^{*,‡,||}

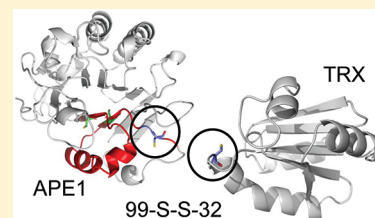
[†]Section of Pediatric Hematology and Oncology, Department of Pediatrics, and [‡]Department of Biochemistry and Molecular Biology, Indiana University School of Medicine, Indianapolis, Indiana 46202-3082, United States

[§]Department of Chemistry, Washington University in St. Louis, St. Louis, Missouri 63130, United States

^{||}Department of Chemistry and Chemical Biology, Purdue School of Science, Indiana University-Purdue University Indianapolis, Indianapolis, Indiana 46202, United States

S Supporting Information

ABSTRACT: Apurinic/apyrimidinic endonuclease (APE1) is an unusual nuclear redox factor in which the redox-active cysteines identified to date, C65 and C93, are surface inaccessible residues whose activities may be influenced by partial unfolding of APE1. To assess the role of the five remaining cysteines in APE1's redox activity, double-cysteine mutants were analyzed, excluding C65A, which is redox-inactive as a single mutant. C93A/C99A APE1 was found to be redox-inactive, whereas other double-cysteine mutants retained the same redox activity as that observed for C93A APE1. To determine whether these three cysteines, C65, C93, and C99, were sufficient for redox activity, all other cysteines were substituted with alanine, and this protein was shown to be fully redox-active. Mutants with impaired redox activity failed to stimulate cell proliferation, establishing an important role for APE1's redox activity in cell growth. Disulfide bond formation upon oxidation of APE1 was analyzed by proteolysis of the protein followed by mass spectrometry analysis. Within 5 min of exposure to hydrogen peroxide, a single disulfide bond formed between C65 and C138 followed by the formation of three additional disulfide bonds within 15 min; 10 total disulfide bonds formed within 1 h. A single mixed-disulfide bond involving C99 of APE1 was observed for the reaction of oxidized APE1 with thioredoxin (TRX). Disulfide-bonded APE1 or APE1–TRX species were further characterized by size exclusion chromatography and found to form large complexes. Taken together, our data suggest that APE1 is a unique redox factor with properties distinct from those of other redox factors.



Cells are continually subjected to reactive oxygen species resulting from normal metabolic processes as well as from exogenous sources and have in place mechanisms to repair damage to cellular components (reviewed in ref 1). Oxidative damage to proteins, which can lead to loss of function through the formation of disulfide bonds, is repaired by general redox factors such as thioredoxin or glutaredoxin or, in the case of nuclear proteins, by the multifunctional DNA repair and redox factor apurinic/apyrimidinic endonuclease (APE1) or Ref-1.²

APE1 is a multifunctional protein that serves as an essential base excision repair protein and, as a nuclear redox factor, regulates the activity of a number of important transcription factors (reviewed in ref 2). Its role in regulating transcriptional activity through a redox mechanism was first established for AP-1 (c-Jun/c-Fos)^{3,4} and later shown for a number of other transcription factors, including NF- κ B,^{5–7} HIF-1 α ,⁸ and p53.⁹ The idea that AP-1 may be under redox regulation in the cell came in part from the observation that the oncogene v-Jun with a Cys to Ser substitution in the DNA-binding domain of the protein was no longer under cellular regulation. This finding suggested that redox regulation of AP-1 might be mediated by a thiol exchange mechanism. Of the seven Cys residues present in APE1, a single Cys-to-Ala substitution, C65A, resulted in the loss of APE1's redox activity.¹⁰ In this same study, oxidized

C93A APE1 was shown to retain redox activity. We found in previous studies that none of the oxidized APE1 mutants retained redox activity; however, the reduced C93A APE1 was significantly less redox-active than wild-type APE1, while C65A APE1 was completely redox-inactive.¹¹

We next examined the conservation of Cys residues in vertebrates and discovered that Cys 65 is conserved only in mammals; the residue in zebrafish APE equivalent to Cys 65 is Thr 58.¹² Through substitution of Thr 58 with a Cys residue (T58C), zebrafish APE gains redox function both in redox EMSAs and in cell-based transactivation assays; wild-type zebrafish APE1 retains repair activity but lacks redox activity.¹¹ Additionally, redox-active T58C zebrafish APE1 was inhibited by an APE1 redox specific small molecule.¹¹ Of the seven cysteines in human APE1, all except Cys 65 and Cys 138 are conserved in zebrafish APE, but no disulfide bonds are observed in the crystal structures of zebrafish APE¹¹ or human APE1.^{11,13–15} In fact, none of the cysteines are

Received: July 5, 2011

Revised: November 5, 2011

Published: December 8, 2011



positioned appropriately or close enough to form intramolecular disulfide bonds in either protein.

The first question we sought to answer in this study is what role, if any, the five remaining Cys residues (other than C65 and C93) play in APE1's redox activity. We next examined the role of APE1's redox activity in cell growth by characterizing growth for cells expressing redox-active versus redox-impaired APE1. As a redox factor, APE1 is necessarily oxidized and subsequently reduced by a cellular redox factor, such as thioredoxin (TRX). Therefore, we examined disulfide bond formation in oxidized APE1 alone or reacted with TRX. Finally, we further characterized disulfide-bonded APE1 and APE1-TRX species by size exclusion gel chromatography.

■ EXPERIMENTAL PROCEDURES

Preparation of Proteins and Mutants. Mutations resulting in the C65A, C93A/C99A, C93A/C138A, C93A/C208A, C93A/C296A, and C93A/C310A substitutions were introduced into hAPE1 encoded within a pGEX-3X vector through site-directed mutagenesis by using the Stratagene Quikchange kit and confirmed by DNA sequencing. GST-APE1 proteins were expressed and purified as previously described.¹¹

APE1 mutants, including only specific Cys residues with all others as Ala, C65, C65/C93, C65/C99, C93/C99, and C65/C93/C99 APE1 were introduced through site-directed mutagenesis into an N-terminal hexa-His SUMO fusion (Invitrogen; Rockville, MD) by using the Stratagene Quikchange kit and confirmed by DNA sequencing. These proteins were expressed and purified, as previously reported for wild-type APE1, by using Ni-NTA affinity chromatography, on-column Ulp1 cleavage, followed by SP-Sepharose ion exchange chromatographic separation.¹⁶

The thioredoxin mutant, including only C32 (TRXC32) with Cys 35 mutated to Ser and all other Cys residues mutated to Ala, was created by using site-directed mutagenesis of a plasmid encoding TRX cloned into pET15b and confirmed by DNA sequencing. TRXC32 was expressed and purified as previously described for thioredoxin.¹⁶

For transactivation assays, mutations were introduced through site-directed mutagenesis in the pcDNA-wtAPE1 vector by using the Stratagene Quikchange kit and confirmed by DNA sequencing. The following mutants were generated: C65A, C93A, C99A, C138A, C208A, C93A/C99A, C93A/C99A/C138A, and C93A/C99A/C138A/C208A.

Electrophoretic Mobility Shift Assay (EMSA). EMSAs were performed as described previously¹² with the following modifications. Purified APE1 (0.3 mM) and its mutant proteins were reduced with 1.0 mM DTT for 10 min and diluted to a final concentration of 0.006 mM with 0.02 mM DTT in PBS. Reduced APE1 (2 μ L) or its mutant proteins were added to EMSA reaction buffer [10 mM Tris (pH 7.5), 50 mM NaCl, 1 mM MgCl₂, 1 mM EDTA, and 5% (v/v) glycerol] with 2 μ L of a 0.007 mM protein mixture (1:1) of purified truncated c-Jun and c-Fos proteins containing the DNA-binding domain and leucine zipper region in a total volume of 18 μ L and incubated for 30 min at room temperature. The EMSA was performed as previously described.^{12,16,17}

Transactivation Assays. Skov-3X cells containing the NF κ B-Luc gene reporter were cotransfected with a control pcDNA empty vector plasmid, pcDNA-wtAPE1 or pcDNA-APE1 mutants, and a *Renilla* luciferase control reporter vector, pRL-CMV (Promega Corp., Madison, WI), in a 1:10 ratio

using lipofectamine TM 2000. After being transfected for 30 h, cells were lysed, and the *Firefly* and *Renilla* luciferase activities were assayed using the Dual Luciferase System (Promega Corp.) with *Renilla* luciferase activity for normalization in a 96-well microtiter plate luminometer (Thermolabs systems, Franklin, MA). All of the transfection experiments were performed in triplicate and repeated at least three times as independent experiments.

Enzyme Kinetic Assays. The AP endonuclease activity for recombinant proteins APE1 and APE1 C65/C93/C99 was measured in a fluorescence-based kinetic assay by using a duplex DNA substrate containing a tetrahydrofuran abasic site mimic as the substrate. The assay employs fluorescein and dabcyI as a fluor-quench pair in oligonucleotides 5'-6-FAM-GCC GAC FGA GGA CGT ACG CG-3' and 5'-CGC GTA CGT CCT CTG TCG GC-Q-3' from Eurogentec Ltd. (San Diego, CA),^{18,19} where FAM indicates fluorescein and Q indicates dabcyI. The oligonucleotides were diluted in water to a final concentration of 100 μ M and annealed in a 4:5 ratio of fluorescein-labeled to dabcyI-labeled oligonucleotides. Release of the fluorescein-labeled oligonucleotide following cleavage at the abasic site by an AP endonuclease was achieved by thermal denaturation at 37 °C and followed in the kinetic mode with a Tecan Ultra 384 instrument using an excitation wavelength of 485 nm and an emission wavelength of 535 nm. APE1 and APE1 C65/C93/C99 were assayed in 50 mM Tris (pH 7.5), 125 mM NaCl, 1 mM MgCl₂, and 0.8% DMSO. Optimal concentrations of 0.04 nM APE1 and 0.06 nM APE1 C65/C93/C99 were determined by varying the enzyme concentration at a fixed substrate concentration of 25 nM. The substrate was then varied from 0 to 75 nM to determine V_{\max} and K_m values for this enzyme. DMSO was included in the assay in preparation for screening of small-molecule inhibitors dissolved in 0.8% DMSO and found not to affect the activity of the enzyme. Kinetic parameters were calculated from the average of quadruplicate measurements for each substrate concentration using the Enzyme Kinetics module in SigmaPlot (SigmaPlot 11.2).

E3330 Inhibition Assay. E3330 was preincubated with 2 μ L of purified APE1 and substituted proteins reduced as described above in EMSA reaction buffer in a total volume of 16 μ L for 30 min, and the EMSA was performed as previously described.¹²

Cell Growth and Proliferation Assays. Cell growth and proliferation were assessed using the xCELLigence DP System (Roche Applied Science, Indianapolis, IN), as previously described.^{12,19-21} Briefly, Panc1 cells were transfected with a pcDNA empty vector, pcDNA-wtAPE1 or pcDNA-APE1 mutants, using lipofectamine TM 2000 in two 16-well plates of the xCELLigence DP System. After transfection for 4 h, fresh medium with fetal bovine serum (FBS) was added to the transfected cell cultures to yield a final FBS concentration of 10%. Cell growth was monitored continuously and recorded as a cell index every 30 min for 66 h. The cell index was normalized to the 1 h time point in the xCELLigence analysis. The assays were performed in duplicate and repeated at least three times in independent experiments.

Oxidation of APE1 and Reaction with TRXC32. Samples (200 μ L) of 10 μ M wild-type APE1 and APE1 C65/C93/C99 in 10 mM Tris (pH 8.0) were treated with 1 mM H₂O₂ for 1, 5, or 15 min at room temperature. A fourth sample of wild-type APE1 was incubated under the same conditions for 30 min, at which time the sample was split into two separate samples. One

sample of 10 μ M APE1 was incubated for an additional 30 min (60 min total) in 1 mM H_2O_2 and then the reaction quenched with NEM at a final concentration of 2 mM for 15 min prior to the mixture being frozen at -80°C . The second sample of 10 μ M APE1 was incubated with 10 μ M TRXC32 for 30 min and then the reaction quenched with NEM, at a final concentration of 2 mM, for 15 min prior to the mixture being frozen at -80°C . Two independent experiments were performed for the oxidation of APE1 with H_2O_2 and subsequent reaction with TRXC32; for both experiments, the same result was obtained.

LC-ESI-MS/MS Analysis of Protein Digests. Ten microliters of a 10 μ M protein sample was diluted to 50 μ L with 10 mM Tris-HCl (pH 8.0) buffer, and the diluted protein sample was digested using a protein:trypsin ratio of 50:1 at 37°C for 16 h. The digestion reaction was quenched by addition of 1 μ L of concentrated acetic acid. Three independent replicates of the digestion experiment were performed. The digestion solution from each digestion replicate was then analyzed by LC-MS/MS whereby 5 μ L of the quenched digestion solution was loaded onto a Dionex Acclaim PepMap Nano trap column and desalted with 0.1% formic acid at a rate of 8 μ L/min for 7 min. Peptides were then separated by using a silica capillary column with a PicoFrit tip (New Objective, Inc., Woburn, MA) by using a linear gradient supplied by a Dionex Ultimate 3000 instrument (Dionex, Sunnyvale, CA) and run at a rate of 260 nL/min from 20 to 55% acetonitrile, with 0.1% formic acid, over 70 min. The silica capillary was custom packed with C18 reverse phase material (Magic, 0.075 mm \times 150 mm, 5 μ m, 120 \AA , Michrom Bioresources, Inc., Auburn, CA). The flow was directed by a PicoView Nanospray Source (PV550, New Objective, Inc.) into an LTQ FTICR mass spectrometer (Thermo-Scientific, San Jose, CA) with a spray voltage of 1.8–2.0 kV and a capillary voltage of 27 V. The LTQ FTICR was operated in standard data-dependent acquisition mode controlled by Xcalibur version 2.0.7. Peptide mass spectra (m/z range of 300–2000) were acquired at a high mass resolving power (100000 for ions at m/z 400). In the data-dependent mode, the six most abundant multiply charged ions with a minimal intensity of 1000 counts were subjected to collision-induced dissociation (CID) in the linear ion trap. Precursor activation in CID was performed with an isolation width (m/z) of 1, an activation time of 30 ms, and a normalized collision energy of 35% of the maximum. The LTQ FTICR was externally calibrated using a standard mixture of caffeine, MRFA, and Ultramark 1621. The mass calibration was checked and repeated before the LC-MS experiments to optimize the accuracy of the mass measurements.

Search for and Analysis of Disulfide Bonds. The MS/MS *.raw data files were converted to *.mgf files with DTASuperCharge (version 2.0a6 from the open source proteomics platform MSQuant, version 2.0a81)²² and then submitted to MassMatrix, a custom search engine developed by Xu et al.^{23–25} The enzyme was set to “trypsin”. The maximal number of missed cleavages was 2. The peptide mass tolerance was 5 ppm, allowing for one ^{13}C peak. The peptide charge was allowed to be +1, +2, or +3. The product-ion mass tolerance was 0.8 Da. The variable modifications chosen were NEM modification of cysteine and oxidation of methionine. The product-ion (MS/MS) spectra of all of the identified disulfide-containing peptide ions from the MassMatrix search were further manually inspected, and only those whose spectra were consistent with the assigned peptide were used.

Preparation and Purification of APE1 C99–TRXC32 Disulfide-Bonded Species.

For this experiment, an N-terminally truncated version of APE1, including only Cys 99 with all other Cys residues mutated to Ala ($\Delta 40\text{APE1 C99}$), was used. As described above for other APE1 mutants, site-directed mutagenesis with the Stratagene Quikchange kit was used to introduce mutations, which were confirmed by DNA sequencing. The protein was expressed and purified as previously described.^{12,26} A sample of 200 μ L of 100 μ M $\Delta 40\text{APE1 C99}$, 1 mM diamide, 10 mM Tris-HCl (pH 8.0), and 0.1 M NaCl was incubated at room temperature for 30 min and then dialyzed against 10 mM Tris-HCl (pH 8.0) and 0.1 M NaCl at 4°C overnight; 200 μ L of 2 mM TRXC32, 1 mM DTT, 10 mM Tris-HCl (pH 8.0), and 0.1 M NaCl was incubated at room temperature for 30 min and then dialyzed against 10 mM Tris-HCl (pH 8.0) and 0.1 M NaCl at 4°C overnight. The TRXC32 sample was diluted to 1 mL with 10 mM Tris-HCl (pH 8.0) and 0.1 M NaCl, incubated with 0.5 mL of Ni-NTA agarose beads at 4°C for 1 h by nutating, washed thoroughly with 10 mM Tris-HCl (pH 8.0), 0.1 M NaCl, and 20 mM imidazole, and then incubated with the $\Delta 40\text{APE1 C99}$ sample overnight at 4°C by nutating. The Ni-NTA beads with TRXC32 and $\Delta 40\text{APE1 C99}$ samples were washed thoroughly with 10 mM Tris-HCl (pH 8.0), 0.1 M NaCl, and 20 mM imidazole, followed by elution with 10 mM Tris-HCl (pH 8.0), 0.1 M NaCl, and 250 mM imidazole. The result was analyzed on a nonreducing SDS-PAGE gel. The $\Delta 40\text{APE1 C99}$ –TRXC32 disulfide-bonded species was further purified by size exclusion chromatography using a Superdex 200 column run in 50 mM Tris (pH 8.0) and 0.5 M NaCl.

RESULTS

Identification of Redox-Active Cys Residues in APE1.

We and others demonstrated that Cys 65 is required for the redox activity of APE1 and that Cys 93 also participates in the redox activity.^{12,27} To determine whether other Cys residues might be involved in the redox activity of APE1, we analyzed double-Cys mutants including C93A and substitutions of the other Cys residues, excluding Cys 65. APE1 C65A is redox-inactive; thus, any additional involvement of Cys residues in the redox activity would be masked in the context of this mutant. The selection of double mutants including C93A was based on the finding that the redox activity of C93A-substituted APE1, as assessed by redox EMSA analysis and cell-based transactivation assays, is approximately 50% of that of the wild-type protein, whereas individual substitution of Cys residue 99, 138, 208, 296, or 310 had no significant effect on redox activity.¹¹ Therefore, C99, C138, C208, C296, and C310 were individually substituted with Ala along with C93 to create double mutants. The substituted APE1 proteins were tested for their ability to reduce c-Jun/c-Fos, which then binds DNA, resulting in a shifted band in a redox EMSA. Of the double-Cys mutants, all but C93A/C99A retained 50–60% of the redox activity. As the C93A mutant alone retains approximately 50% of the activity, the additional substitutions did not further reduce the redox activity. However, the redox activity of the C93A/C99A enzyme was reduced to $\sim 10\%$ of the wild-type activity in this analysis, indicating a significant loss of redox activity (Figure 1A,B).

To confirm the results of *in vitro* redox EMSAs, the C93A/C99A double mutant was compared to a subset of single mutants in a cell-based transactivation assay in which luciferase activity is dependent upon reduction and binding of NF- κ B, a

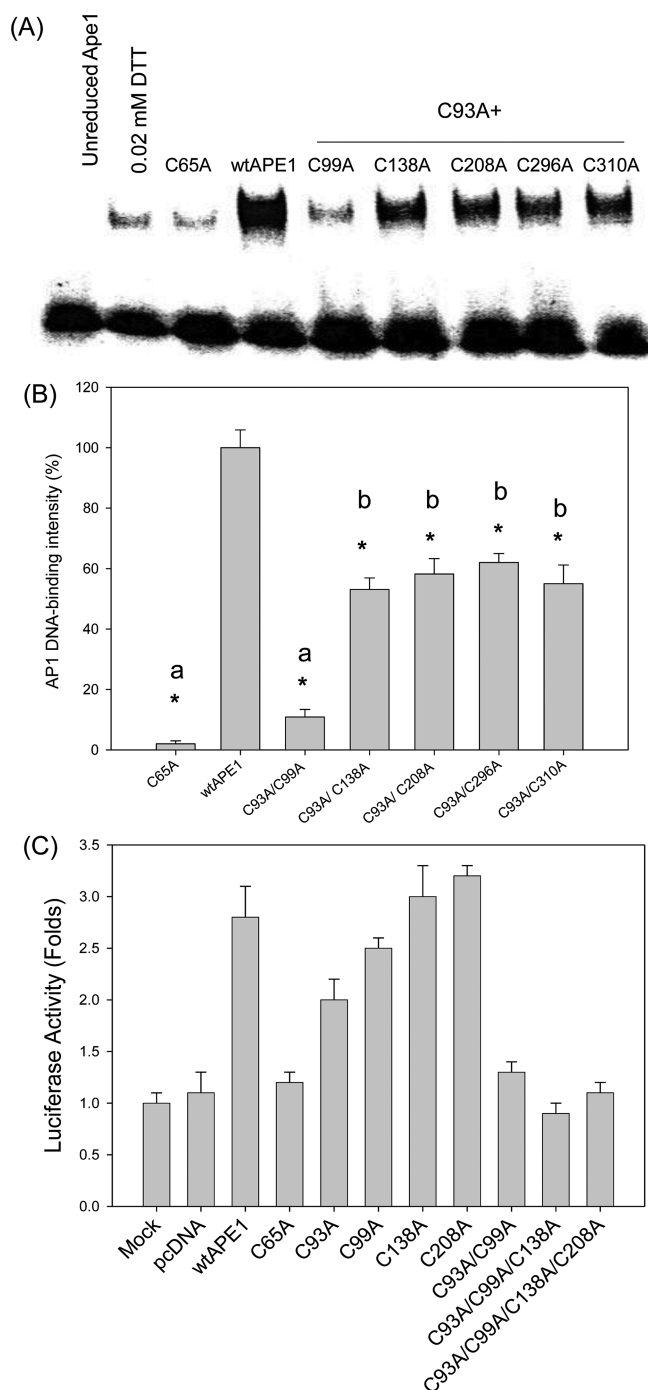


Figure 1. (A) Redox EMSA for double-Cys mutants including C93A. Reduced APE1 and its mutant proteins (reduced with 1 mM DTT and then diluted to a final DTT concentration of 0.02 mM) or oxidized (unreduced) proteins were preincubated with purified truncated AP-1 protein (c-Jun/c-Fos) for 30 min, and then the EMSA was performed as previously described.^{12,16,17} For the control lane, 0.02 mM DTT was used as a control for the DTT that is carried over from the protein reduction (lane 2). Unreduced wild-type (wt) APE1 protein (lane 1) and mutant proteins (data not shown) did not show redox activity. Reduced wt APE1 enhanced the DNA binding of AP-1 (lane 4), whereas reduced C65A APE1 and double-Cys mutant C93A/C99A APE1 did not (lanes 3 and 5). All other double-Cys mutants including C93A retain 50–60% of the redox activity (lanes 6–9). (B) Quantitation of the results of the experiments shown in panel A. Data are means \pm the standard error from three independent experiments, and Student's *t* tests were performed. Asterisks denote a

Figure 1. continued

significant difference at the $p < 0.05$ level compared with wt APE1, whereas a and b indicate there is no significant difference between the samples labeled a and among the samples labeled b, respectively. (C) Results of a transactivation assay comparing C93A/C99A to other mutants. Transactivation assays were performed as described in Experimental Procedures and as previously described.¹² All of the transfection experiments were performed in triplicate and repeated at least three times in independent experiments. Data are means \pm the standard deviation from one representative experiment. The C93A mutant has reduced activity compared to wt APE1, whereas C99A, C138A, and C208A mutants have activity close to that of the wild type. The C93A/C99A double mutant was redox-inactive with activity comparable to that of the C65A mutant. No further reduction in activity was observed for the C93A/C99A/C138A triple mutant or the C93A/C99A/C138A/C208A quadruple mutant.

known APE1 redox target, to its target DNA binding sequence.¹² In this assay, as shown in Figure 1C, the C93A mutant has diminished activity compared to wt APE1 while C99A, C138A, and C208A have activity close to that of the wild type. The C93A/C99A double mutant was redox-inactive in this assay with a loss of activity comparable to that of the C65A mutant. The C93A/C99A/C138A triple mutant and the C93A/C99A/C138A/C208A quadruple mutant were also redox-inactive in the transactivation assay. Thus, these results suggest that three Cys residues are involved in the redox activity of APE1, C65, C93, and C99.

Three Cys Residues Are Necessary and Sufficient for Redox Activity in APE1. To determine whether C65, C93, and C99 are sufficient for redox activity in APE1, we constructed and expressed APE1 that has only these Cys residues (APE1 C65/C93/C99). All other Cys residues were substituted with Ala (i.e., C138A, C208A, C296A, and C310A). APE1 C65/C93/C99 was then tested for redox activity in the redox EMSA and cell-based transactivation assays and found to retain wild-type redox activity, as shown in Figures 2 and 3. We next analyzed single-Cys mutants introduced within APE1 C65/C93/C99 to assess the contributions of each Cys residue to the redox activity of APE1. To do this, we introduced substitutions resulting in APE1 that has only two Cys residues, C65/C93, C65/C99, or C93/C99; for these proteins, C99, C93, or C65 was substituted with Ala, respectively. The mutant APE1 proteins were then tested for redox activity in the redox EMSA and cell-based transactivation assays (Figures 2 and 3). Of these, C65/C93 and C65/C99 both showed decreases of $\sim 50\%$ in redox activity compared to wild-type or APE1 C65/C93/C99 activity, whereas APE1 C93/C99 was redox-inactive. The activity measured for APE1 C65/C99 is consistent with the results we obtained previously for the C93A mutant.¹² Further, the decrease in redox activity observed for APE1 C65/C93 confirms a role in the redox activity for Cys 99, as suggested by the double-mutant experiments discussed above. Finally, we assessed APE1 including a single Cys residue, APE1 C65, for redox activity. In both the redox EMSA and transactivation assays, APE1 C65 was redox-inactive, equivalent to the APE1 C93/C99 enzyme. Thus, a single Cys residue is not sufficient to confer redox activity. These results provide more evidence that C65, C93, and C99 are all involved in the redox activity of APE1.

It is also of interest to determine whether substitution of C138, C208, C296, and C310 in the APE1 C65/C93/C99 enzyme affects the endonuclease activity of the enzyme. In a

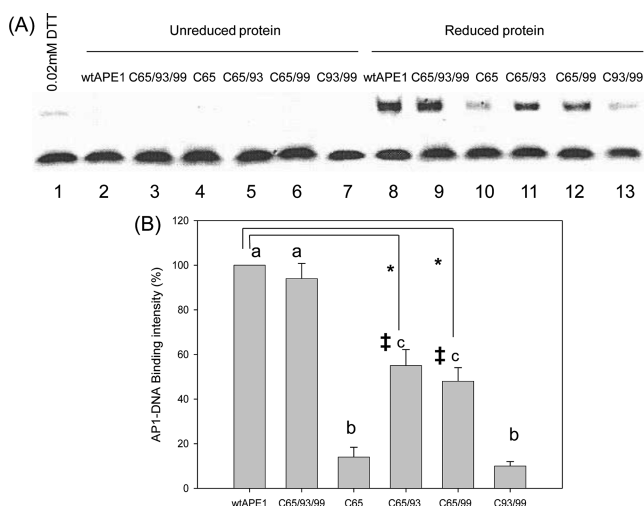


Figure 2. EMSA redox activity for APE1 including C65, C93, and C99 and its mutants. (A) An EMSA was performed as described in Experimental Procedures. DTT (0.02 mM) was the control for DTT carryover (lane 1). Oxidized proteins (lanes 2–7) did not enhance AP-1–DNA binding. Reduced APE1 C65/C93/C99 and wt APE1 (lanes 8 and 9) or APE1 C65 (lanes 10 and 13) did not, whereas APE1 C65/C93 and APE1 C65/C99 (lanes 11 and 12) demonstrated a weakened but intermediate binding pattern. (B) Quantitation of the results of the EMSA. Data are means \pm the standard error from three independent experiments, and Student's *t* tests were performed. Asterisks and double daggers indicate a significant difference at the *p* < 0.05 level compared with wt APE1 and APE1 C65, respectively, whereas a–c indicate there is no significant difference (*p* > 0.05) between samples labeled a, between samples labeled b, and between samples labeled c, respectively.

steady state kinetic analysis, similar K_m values of 9.3 and 17.9 nM and V_{max} values of 123000 and 110000 relative fluorescence units $\mu\text{g}^{-1} \text{s}^{-1}$ were determined for the wild-type and C65/C93/C99 enzymes, respectively (Figure 4). Thus, the C65/C93/C99 enzyme retains near wild-type endonuclease activity, suggesting that the Cys residues that were substituted with Ala do not contribute significantly to the endonuclease activity of APE1. Both C65/C93 and C65/C99 enzymes also retain wild-type endonuclease activity.²⁸ To test whether the substitutions affect the protein structure, we measured the CD spectra and found they are similar (Figure 1 of the Supporting Information) to that of the wild-type protein, suggesting that they retain a native-like state.

Effect of the Redox Inhibitor E3330 on APE1 and Its Mutants. To assess further the redox properties of APE1 C65/C93/C99 and its mutants, we examined the inhibition of redox activity by (E)-3-[2-(5,6-dimethoxy-3-methyl-1,4-benzoquinonyl)]-2-nonylpropenoic acid (E3330). E3330 was previously shown to inhibit specifically the redox function of APE1.^{11,12,17,26} Using E3330 in EMSA experiments, as shown in Figure 5, we determined that E3330 blocks the redox activity of APE1 C65/C93/C99, APE1 C65/C93, APE1 C65/C99, and wt APE1 in a dose-dependent manner; the IC_{50} values are 18.8, 21.7, 18.9, and 17.4 μM , respectively. The ability of E3330 to inhibit the redox activity of APE1 C65/C93/C99 as well as redox-active APE1 C65/C93 and C65/C99 mutants at similar IC_{50} values versus that of wild-type APE1 suggests that all of these enzymes reduce AP-1 by a similar mechanism.

Effect of APE1 Cys Mutants on Cell Proliferation in Panc1 Cells. To determine the effect of APE1's redox activity

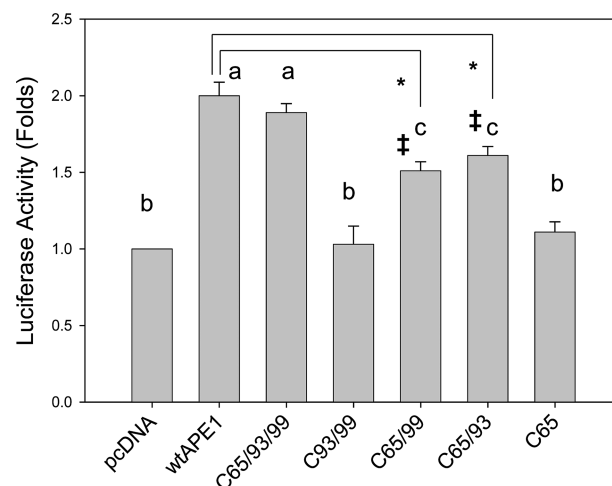


Figure 3. Cell-based transactivation data for wt APE1 and Cys-restricted mutants. Skov-3X cells containing the NF- κ B luciferase reporter construct were transfected with plasmid pcDNA-wtAPE1 or the mutant APE1 (pcDNA-C65/C93/C99, pcDNA-C93/C99, pcDNA-C65/C93, pcDNA-C65/C99, and pcDNA-C65) and a *Renilla* luciferase control reporter vector pRL-CMV. After a 30 h transfection period, cells were lysed, and *Firefly* and *Renilla* luciferase activities were assayed using *Renilla* luciferase activity for normalization. All of the transfection experiments were performed in triplicate and repeated at least three times in independent experiments. Data are means \pm the standard error from three independent experiments, and Student's *t* tests were performed. Asterisks and double daggers indicate a significant difference at the *p* < 0.05 level compared with wt APE1 and the control sample (pcDNA), respectively, whereas a–c indicate there is no significant difference (*p* > 0.05) between samples labeled a, among samples labeled b, and between samples labeled c, respectively.

on the stimulation of cell proliferation, we compared the growth of cells transfected with pcDNA-wtAPE1, pcDNA-APE1 Cys mutants, or pcDNA (Figure 6). APE1 mutants include those analyzed for redox activity. Redox-inactive mutants include C65A, C65 only, or C93/C99 only, redox-impaired mutants C65/C93 or C65/C99 only, and redox-active mutant C65/C93/C99. Cell growth was monitored by using the xCELLigence DP system (Figure 6), for which data were obtained every 30 min for 66 h. Redox-active mutant APE1 C65/C93/C99 stimulated cell growth that was comparable to that of wt APE1, whereas the redox-impaired mutants did not stimulate cell growth and, in fact, had slower cell growth comparable to or slower than that observed for the control pcDNA vector. The redox-inactive mutants, C65A and C93/C99 only, showed slower cell growth compared to that of the control pcDNA vector. These results confirm an important role for the redox activity of APE1 in stimulating growth of cells, in this case Panc1 cells.

Disulfide Bond Formation in APE1. Thiol-mediated redox reactions necessarily involve the formation of disulfide bonds in the redox factor, which is oxidized in the process of reducing another protein. Oxidized APE1 is then reduced by another cellular redox factor such as thioredoxin.²⁹ Here, we report LC–MS/MS analysis of trypsin-digested samples to identify both disulfide bonds formed in APE1 following oxidation with H_2O_2 and mixed disulfide bonds formed between oxidized APE1 and thioredoxin. The use of H_2O_2 serves to induce disulfide bond formation^{30–33} through oxidation of Cys residues to sulfenic acid, making them susceptible to nucleophilic attack by a thiolate within the

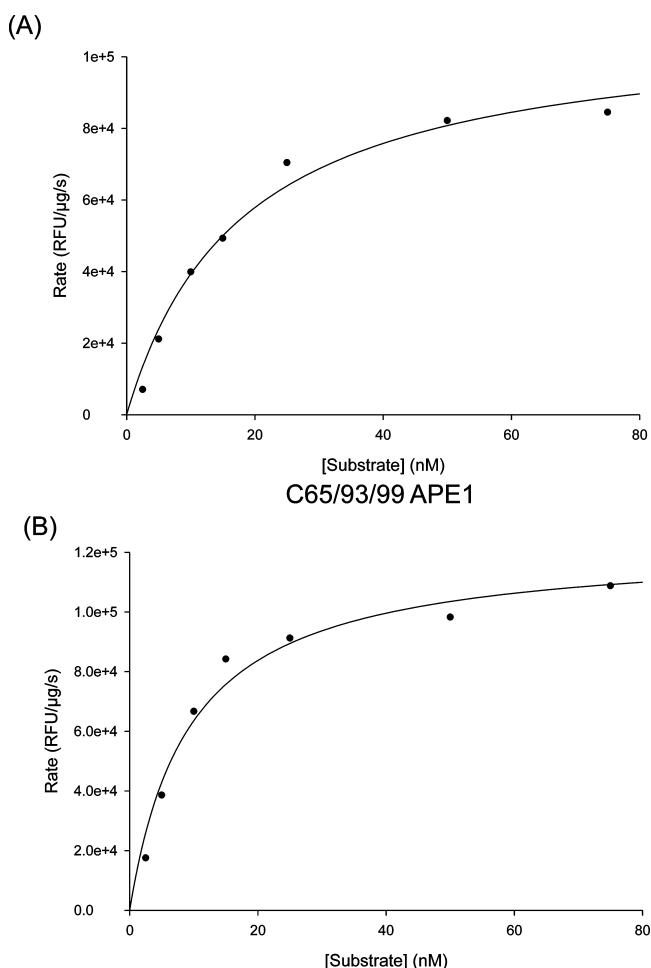


Figure 4. Enzymatic characterization of wild-type APE1 and APE1 C65/C93/C99. A kinetics analysis was performed for C65/93/99 APE1 (A) and wild-type APE1 (B) using a fluorescence-based solution assay adapted from a previously reported assay.¹⁸ In this assay, the concentration of the tetrahydrofuran-containing abasic site substrate mimic was varied from 0 to 75 nM with an enzyme concentration of 0.04 or 0.06 nM for wild-type APE1 or APE1 C65/C93/C99, respectively. The maximal velocity and K_m values were calculated by using the Enzyme Kinetics module in SigmaPlot (SigmaPlot 11.2).

protein; the disulfide-bonded state of APE1 is recognized and reduced by thioredoxin. To trap mixed disulfide bonds involving thioredoxin and APE1, we used an engineered thioredoxin containing only the nucleophilic Cys 32³⁴ (TRXC32). Of the five Cys residues in thioredoxin, all but Cys 32 were substituted with either Ser or Ala (see Experimental Procedures).

Both wild-type APE1 and APE1 C65/C93/C99 were incubated with 1 mM H₂O₂ for 1, 5, 15, or 60 min prior to the reaction being quenched with the irreversible Cys-modifying reagent, *N*-ethylmaleimide (NEM), which prevents disulfide bond scrambling during further sample manipulation. APE1 contains seven Cys residues; thus, there are 21 possible unique disulfide bonds involving two different Cys residues. Of the seven cysteines present in APE1, only C99 and C138 are solvent accessible, with C138 being the most accessible. Disulfide bonds were identified from three independent digests of each sample and analyzed by LC–MS/MS (see Experimental Procedures). Only the disulfide-bonded peptides that were observed in all three replicates for the different time

points and at significant levels are listed in Table 1. The disulfide-bonded peptides were identified by using Mass Matrix, a proteomics engine (see Experimental Procedures) that searches the LC–MS/MS data, and confirmed by manual searching of all cysteine-containing peptides. We were able only to detect the disulfide-bonded peptides and not quantify them because they all respond differently to ESI and their response factors are unknown.

No disulfide bonds were observed for the 1 min sample. After 5 min, a single disulfide bond, C65–C138, was observed in the wild-type APE1 sample. Incubation for 15 min resulted in the formation of four disulfide bonds, C65–C138, C65–C99, C93–C138, and C138–C208, and after 60 min, 10 disulfide bonds were observed (Table 1). In the APE1 C65/C93/C99 sample, no disulfide bonds were observed in the 1 and 5 min samples; a single disulfide bond, C65–C99, was observed after 15 min. All possible disulfide bonds were observed in the 60 min sample, including C65–C93, C93–C99, and C65–C99. Thus, for each sample, the first disulfide bond formed between C65 and a solvent accessible cysteine, C138, in the case of the wild-type protein and C99 in the APE1 C65/C93/C99 protein. Subsequent disulfide bonds formed at later time points in each sample likely involve resolution of the first disulfide bond formed followed by further scrambling of disulfide bonds. Although we can determine which cysteines are involved in the disulfide bonds on the basis of the LC–MS/MS results, we cannot determine whether the disulfide bonds are intermolecular or intramolecular. To assess the possibility of intermolecular disulfide bond formation, APE1 samples treated with H₂O₂ for 60 min were analyzed by nonreducing SDS–PAGE (Figure 7A), and high-molecular mass bands (>135 kDa) were observed, consistent with the formation of intermolecular disulfide bonds leading to large complexes of APE1.

To determine whether a disulfide-bonded species of APE1 is recognized by thioredoxin, we incubated APE1 with 1 mM H₂O₂ for 30 min and then reacted APE1 with TRXC32 for an additional 30 min at room temperature. Following incubation with TRXC32, three new bands were observed on the nonreducing SDS gel, corresponding to ~30, ~60, and >135 kDa (Figure 7A). The ~30 kDa band corresponds to a dimeric species of disulfide-bonded TRXC32. The ~60 and >135 kDa bands likely correspond to mixed disulfide-bonded species, including both APE1 and TRXC32; this conclusion is based on a comparison of the APE1 sample treated with H₂O₂ and control APE1 and TRXC32 samples (Figure 7). We hypothesize that the mixed disulfide-bonded species arise through reaction of TRXC32 with the high-molecular mass species of APE1 observed in the oxidized APE1 sample as the intensity of this band appears to decrease compared to that corresponding to monomeric APE1, which appears to remain constant in a comparison of oxidized APE1 and oxidized APE1 treated with TRXC32 (Figure 7A).

Mixed disulfide bond formation was analyzed for H₂O₂-oxidized APE1 reacted with TRXC32. The same 10 disulfide bonds were observed for APE1 in this reaction as for APE1 treated only with H₂O₂ for 60 min. One mixed disulfide bond was found to form between C99 of APE1 and TRXC32. Formation of a disulfide bond between residues C99 of APE1 and C32 of TRX could result from nucleophilic attack of TRXC32 on an existing disulfide bond involving C99 in APE1, attack of TRXC32 on a sulfenic acid oxidized form of C99, or attack of C99 on an intermolecular disulfide-bonded TRXC32.

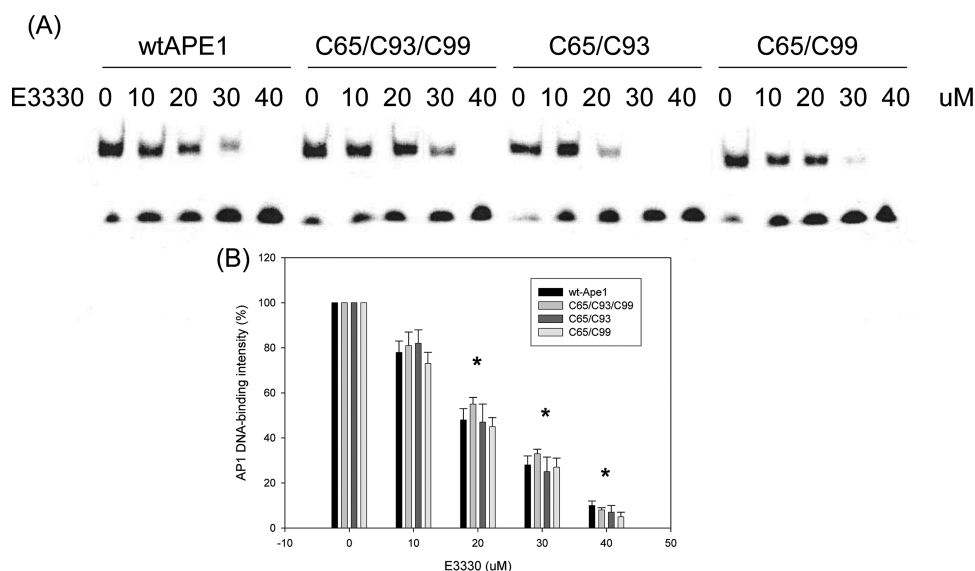


Figure 5. Inhibition of APE1 and minimal Cys mutants as compared to wt APE1 by the small-molecule APE1 redox inhibitor E3330. (A) An increasing amount of E3330 was preincubated with 2 μ L of purified APE1 or its mutant proteins (APE1 C65/C93/C99, APE1 C65/C93, and APE1 C65/C99) (reduced with 1.0 mM DTT and then diluted to 0.006 mM with 0.02 mM DTT in PBS) in EMSA reaction buffer in a total volume 16 μ L for 30 min, and then the EMSA was performed. E3330 inhibited AP-1–DNA binding enhanced by APE1 C65/C93/C99, APE1 C65/C93, APE1 C65/C99, and wt APE1 in a dose-dependent manner. (B) Quantitation of the results of the experiments described above. The redox activity of APE1 C65/C93/C99, APE1 C65/C93, APE1 C65/C99, and wt APE1 was inhibited by E3330 in a dose-dependent manner with 50% inhibition values of 18.8, 21.7, 18.9, and 17.4 μ M, respectively. Data are means \pm the standard error from three independent experiments, and Student's *t* tests were performed. Asterisks indicate a significant difference at the $p < 0.01$ level compared with the E3330-untreated sample. There is no significant difference ($p > 0.05$) comparing the IC_{50} values of E3330 and the inhibition percentages at each dose of E3330 in APE1 C65/C93/C99, APE1 C65/C93, and APE1 C65/C99 to those in wt APE1.

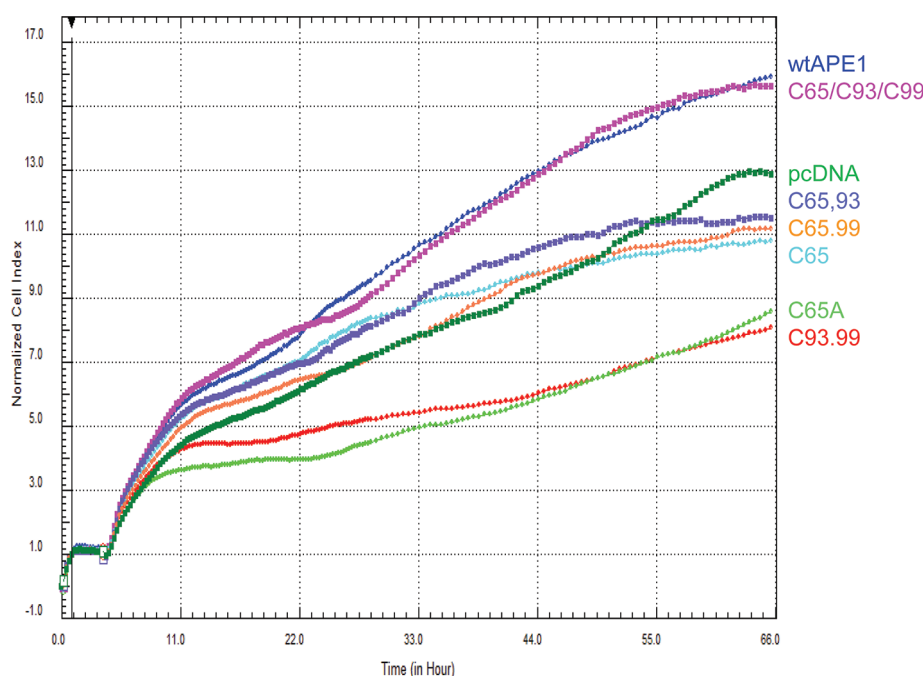


Figure 6. Effect of APE1 and its redox mutants on cell proliferation in Panc1 cells. Panc1 cells were transfected with a control pcDNA empty vector plasmid, pcDNA-wtAPE1 or the pcDNA-APE1 mutants using lipofectamine TM 2000 and analyzed by using the xCELLigence DP System, which measures cell growth in real time. After transfection (4 h), fresh medium with FBS was added. Data were obtained every 30 min for 66 h. Data from one representative experiment are shown. APE1 C65/93/99 stimulated cell growth and proliferation as did wt APE1, similar to what was observed by using an MTT analysis (data not shown). None of the other mutants stimulated growth; some displayed growth levels that were below that observed for the vector control.

As shown in Figure 7A, all of the TRXC32 is in an oxidized form for the sample that reacted with oxidized APE1; there was no detectable band for reduced TRXC32. To characterize

further the APE1–TRXC32 disulfide-bonded complex, we prepared an N-terminally truncated APE1 containing a single Cys residue (Δ 40APE1 C99) to ensure formation of a

Table 1. Time Courses of Disulfide Bond Formation for APE1 Treated with H₂O₂

time (min)	65–138 DB	65–99 DB	65–93 DB	65–296 DB	93–138 DB	93–99 DB	99–138 DB	99–208 DB	138–208 DB	138–296 DB
1										
5	X									
15	X	X			X				X	
60	X	X	X	X	X	X	X	X	X	X

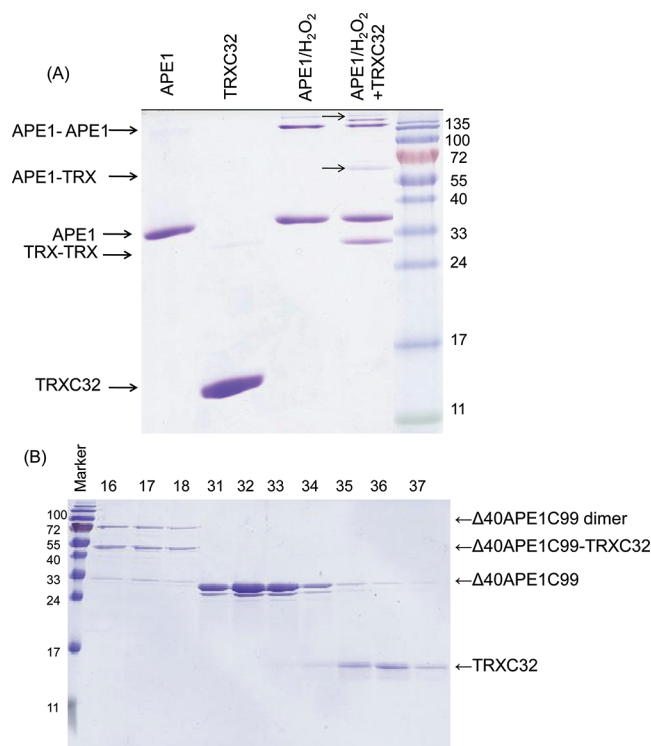


Figure 7. Nonreducing SDS–PAGE analysis of oxidized APE1 with or without TRXC32 (A) and purified disulfide-bonded APE1–TRX samples (B). APE1 was oxidized by using H₂O₂ and then reacted with thioredoxin, including a single Cys, the nucleophilic Cys 32 (TRXC32). Shown in panel A are control samples of APE1 and TRXC32 that were not reacted with H₂O₂, oxidized APE1, and oxidized APE1 that was reacted with TRXC32. APE1 appears to form intermolecular disulfide bonds leading to a product that runs on the gel with an approximate molecular mass of >135 kDa. Reaction with TRXC32 results in the appearance of two new bands (indicated by arrows) corresponding to mixed disulfide-bonded species that run at ~60 and >135 kDa. Shown in panel B are the fractions collected from the size exclusion chromatographic analysis of the Ni-NTA-purified Δ40APE1 C99–TRXC32 disulfide-bonded complex. Fraction numbers are shown at the top of each lane. The void volume for the column, determined by using blue dextran 2000, is 8.0 mL, corresponding to fraction 16. The largest standard protein, thyroglobulin, with a molecular mass of 669 kDa elutes at a volume of 8.95 mL, corresponding to fraction 18. Thus, the apparent molecular mass of the Δ40APE1 C99–TRXC32 complex is greater than 700 kDa based on this calibration. Molecular mass standards for the nonreducing SDS–PAGE analysis are shown in the left-most lane with sizes labeled. The mixed disulfide-bonded species runs on the SDS gel with an apparent molecular mass of ~55 kDa.

homogeneous disulfide-bonded sample. We previously showed that the N-terminally truncated APE1 retains near wild-type redox activity.¹¹ The complex was prepared by treating Δ40APE1 C99 with diazenedicarboxylic acid bis(*N,N*-dimethylamide) (diamide), a thiol oxidizing agent used to induce disulfide bond formation. Oxidized Δ40APE1 C99 was then

reacted with reduced TRXC32. Ni-NTA affinity purification of the complex through use of the hexa-His tag on TRXC32 resulted in samples containing the mixed disulfide product, reduced Δ40APE1 C99, and reduced TRXC32. Via further characterization by size exclusion chromatography, the mixed disulfide-bonded Δ40APE1 C99–TRXC32 species (~55 kDa band on a nonreducing SDS polyacrylamide gel, equivalent to the ~60 kDa product observed for the full-length APE1–TRXC32 sample) eluted from the column close to the void volume along with the dimeric disulfide-bonded Δ40APE1 C99 species. The estimated molecular mass for these disulfide-bonded species is >700 kDa, suggesting that these disulfide-bonded species form very large complexes in solution (Figure 7B). Δ40APE1 C99 and TRXC32 that coeluted with the mixed disulfide-bonded species in the Ni-NTA affinity purification eluted separately on the size exclusion column with apparent molecular masses of ~37 and ~16 kDa, closely matching their calculated molecular masses of 32 and 14 kDa, respectively.

DISCUSSION

Although APE1 has long been recognized as a redox factor, a detailed mechanism for APE1's oxidation and reduction had not yet been reported. In this study, we first identified three cysteine residues (C65, C93, and C99) as necessary and sufficient for APE1's redox activity. The involvement of all three Cys residues was confirmed through further substitution resulting in APE1 enzymes containing only C65 and C93, C65 and C99, or C93 and C99; the first two showed a decrease of ~50% in redox activity, whereas the latter was redox-inactive (Figure 3). In the context of the wild-type APE1 protein, substitution of Cys 99 with Ala does not decrease the redox activity of the protein, whereas for the C65/C93 APE1 protein, a significant loss of redox activity was observed (Figure 1C). These results suggest that other Cys residues within APE1 may partially compensate for the loss of Cys 99 in the C99A mutant. In contrast to thioredoxin, for which two Cys residues, the nucleophilic Cys 32 and resolving Cys 35, are required for redox activity,³⁴ the involvement of three Cys residues in APE1's redox activity indicates a more complex redox mechanism.

We next analyzed a time course of disulfide bond formation upon oxidation of APE1. A single disulfide bond, C65–C138, formed within 5 min of exposure to H₂O₂ in wild-type APE1, and within 15 min, the C65–C99 disulfide bond formed in APE1 C65/C93/C99. As disulfide bond formation involves nucleophilic attack of a thiolate on an oxidized cysteine (a cysteine involved in a disulfide bond or a sulfenic acid form of the residue), a probable explanation for the formation of the single disulfide bond observed in wild-type APE1 is that C138, the most solvent accessible cysteine, was oxidized to a sulfenic acid form and attacked by the thiolate form of C65. Without C138, the single disulfide bond formed in APE1 (C65/C93/C99) may involve a similar attack of C65 on an oxidized C99, also a solvent accessible cysteine (Figure 8). Subsequently, at the 15 min time point, additional new disulfide bonds likely

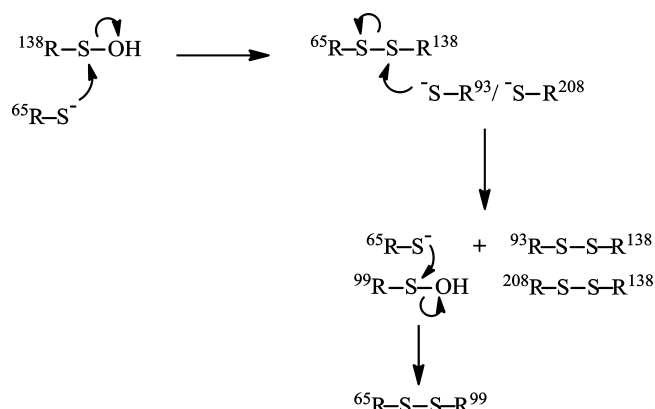


Figure 8. Schematic of a possible mechanism for the formation of disulfide bonds in APE1. Treatment of APE1 with hydrogen peroxide resulted in the formation of a single disulfide bond within 5 min for wild-type APE1 between C65 and C138. Resolution of this disulfide bond through nucleophilic attack by either C93 or C208 would result in two of the four disulfide bonds observed following a 15 min exposure to hydrogen peroxide. This reaction would liberate C65 as a thiolate, which could subsequently attack oxidized C99 and form the fourth disulfide bond that was observed.

result from nucleophilic attack on the original disulfide bond by another thiolate within APE1. This reaction resolves the original disulfide bond and results in the formation of new disulfide bonds. For wild-type APE1, resolution of the initial disulfide bond may involve nucleophilic attack by either C93 or C208, resulting in C93–C138 or C138–C208 disulfide bonds, respectively, releasing C65 as a thiolate to react with oxidized C99 forming the C65–C99 disulfide bond (Figure 8). This cascade of disulfide bond formation is consistent with what is observed for the APE1 (C65/C93/C99) sample in which the C65–C99 bond is first disulfide bond formed. By 60 min, 10 disulfide bonds formed in wild-type APE1, resulting from further resolution of disulfide bonds that were formed at 15 min. The 10 disulfide bonds include the same four observed for the 15 min time point. In APE1 C65/C93/C99, three disulfide bonds formed after 60 min. As the C65–C99 bond formed first, we propose a resolving role for C93 in this protein similar to that seen in the wild-type protein.

In a previous study, we reported disulfide bond formation in $\Delta 40$ APE1, which lacks the 40 N-terminal amino acids, following treatment with E3330 for 1 h at 37 °C. In both control and E3330-treated samples, we observed C65–C93, C65–C99, C93–C99, and C93–C138 disulfide bonds,²⁶ a subset of the disulfide bonds observed in this study for full-length APE1 treated with H_2O_2 at room temperature for 1 h. For the E3330-treated sample, the C65–C138 disulfide bond was also observed.²⁶ The amount of each disulfide bond formed following treatment with E3330 was significantly increased as compared to the control sample based on relative quantitation of each disulfide bond-containing peptide. Thus, the results from our previous study suggest that E3330 acts in a manner similar to that of H_2O_2 in inducing disulfide bond formation in APE1, consistent with our proposal that E3330 reacts transiently with cysteine residues in APE1 making them susceptible to nucleophilic attack.

What we have proposed here is a cascade that is consistent with the formation of the observed disulfide bonds as well as the mutational data in which C65, C93, and C99 are required for redox activity. The cascade is predicated on the initial

disulfide bond formed being susceptible to nucleophilic attack by thiolates in APE1. Within 1 h of oxidation with H_2O_2 , all of the cysteine residues in APE1 were observed in disulfide bonds except C310. The extent of peptide coverage in the LC–MS/MS experiments was overall 80–89%, and all cysteine-containing peptides were observed. There are, of course, other possible mechanisms that could explain the formation of the observed disulfide bonds in APE1. We propose one possible scenario that is consistent with all of the data (Figure 8).

Oxidized APE1 treated with TRXC32 resulted in the formation of a single mixed disulfide bond involving C99 from APE1. Considering the SDS–PAGE analysis of the reaction products and the results from the oxidation studies of APE1, we suggest that the most probable reaction involves nucleophilic attack of TRXC32 on a disulfide bond in APE1 involving C99. Within 15 min, the only disulfide bond involving C99 that forms in APE1 is the C65–C99 disulfide bond; by 60 min, two additional disulfide bonds form, C99–C138 and C99–C208. In this model, thioredoxin would attack one of these disulfide bonds, resulting in the mixed disulfide.

A nonreducing SDS–PAGE analysis of the reaction of APE1 with H_2O_2 suggests that upon oxidation, APE1 forms intermolecular disulfide-bonded species and that these larger complexes most likely react with TRXC32, giving rise to two distinct mixed disulfide-bonded species, one with a molecular mass of ~60 kDa and the other with a molecular mass of >135 kDa (Figure 7). Via further characterization by size exclusion chromatography of the mixed disulfide-bonded species, we find that both the disulfide-bonded $\Delta 40$ APE1 C99– $\Delta 40$ APE1 C99 complex and the mixed disulfide-bonded $\Delta 40$ APE1 C99–TRXC32 species form a very large complex that elutes from a Superdex 200 column with an apparent molecular mass of >700 kDa. The apparent molecular masses of the mixed disulfide-bonded or dimeric disulfide-bonded APE1 were unaltered when it was run at salt concentrations as high as 0.5 M NaCl. $\Delta 40$ APE1 C99 that is not disulfide-bonded to TRXC32 elutes from the Superdex 200 column with an apparent molecular mass of 37 kDa, close to its expected molecular mass of 32 kDa, suggesting that it adopts a native conformation. TRXC32 also elutes with an apparent molecular mass of 16 kDa, close to its expected molecular mass of 14 kDa.

To address the functional significance of the APE1's redox function in the cell, we examined the effect of expressing fully redox-active, redox-impaired, and redox-inactive mutants of APE1 on cell growth in Panc1 cells. In real-time cell growth assays, redox-active APE1 enhanced cell growth as compared to the control. Conversely, redox-impaired or inactive mutants showed either no enhancement or a decreased level of cell growth (Figure 6), consistent with an important functional role for APE1's redox activity in cell growth.

Thus, the results of the time course analysis of disulfide bond formation in both APE1 and the mutants are consistent with a role for C65 as the nucleophilic cysteine, while C93 and C99 likely play roles in resolving disulfide bonds that are formed in APE1 upon oxidation. As a buried residue, C65 is less susceptible to oxidation than the solvent accessible Cys residues C99 and C138. However, to serve as a nucleophile in the formation of a disulfide bond, it must become accessible. This can occur through local unfolding, which we characterized in a study of the interaction of E3330 with APE1 where we discovered that APE1 exists in both native and partially unfolded conformations.²⁶ In the partially unfolded conformation of APE1, C65 would be accessible, consistent with the

disulfide-bonding results. It has also been reported that the region including residues 80–85 that buries C65 in the structure has higher than average *B* factors consistent with greater mobility in this region of the structure,¹⁴ allowing accessibility to C65.

The redox-active Cys residues are clustered in one of the two β -sheets that make up the β -sandwich fold of the APE1 structure. C65 and C93 are located within adjacent strands in the middle of one of the β -sheets within APE1, albeit positioned on opposite sides of the sheet, while C99 is located within a connecting loop region (Figure 9). The distinct

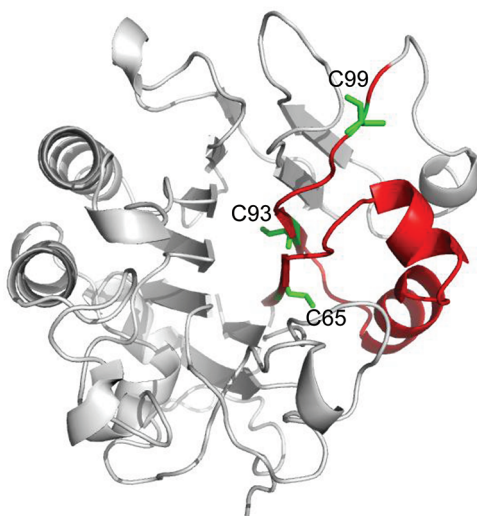


Figure 9. APE1 structure with redox-active cysteines highlighted. A ribbon rendering of APE1 is colored gray, with C65, C93, and C99 shown as green sticks in a view showing the two β -sheets that comprise the β -sandwich fold. The two β -strands containing C65 and C93 along with the intervening helical element and the connecting loop region containing C99 are colored red.

properties of APE1 involving three Cys residues, the potential involvement of intermolecular disulfide bonds, and the formation of a large complex upon mixed disulfide bond formation with thioredoxin distinguish APE1 from other redox factors and suggest a unique redox mechanism.

■ ASSOCIATED CONTENT

■ Supporting Information

CD spectra of wild-type APE1, APE1 C65/C93, and APE1 C65/C99. This material is available free of charge via the Internet at <http://pubs.acs.org>.

■ AUTHOR INFORMATION

Corresponding Author

*M.M.G.: telephone, (317) 278-8486; fax, (317) 274-4686; e-mail, mgeorgia@iupui.edu. M.R.K.: telephone, (317) 274-2755; fax, (317) 274-5378; e-mail, mkelley@iupui.edu.

Funding

This work was supported by National Institutes of Health (NIH) Grant CA114571 to M.M.G., NIH Grants CA121168, CA114571, and CA121168S1 and a Riley Children's Foundation grant to M.R.K., and National Center for Research Resources Grant 2P41RR000954 to M.L.G.

■ ACKNOWLEDGMENTS

We thank Sarah Delaplane in the Georgiadis laboratory for technical assistance in the preparation of APE1 samples and kinetic analyses, Dr. Melissa Fishel for help in construction of the various APE1 Cys mutants, and Drs. Quyen Hoang, Wei Wang, and Jingling Liao for assistance with CD experiments.

■ ABBREVIATIONS

APE1, apurinic/apyrimidinic endonuclease; E3330, (E)-3-[2-(5,6-dimethoxy-3-methyl-1,4-benzoquinonyl)]-2-nonylpropionic acid; ESI-MS, electrospray ionization mass spectrometry; FBS, fetal bovine serum; NEM, *N*-ethylmaleimide; diamide, diazenedicarboxylic acid bis(*N,N*-dimethylamide); PBS, phosphate-buffered saline; SDS–PAGE, sodium dodecyl sulfate–polyacrylamide gel electrophoresis.

■ REFERENCES

- (1) Trachootham, D., Lu, W., Ogasawara, M. A., Nilsa, R. D., and Huang, P. (2008) Redox regulation of cell survival. *Antioxid. Redox Signaling* 10, 1343–1374.
- (2) Luo, M., He, H., Kelley, M. R., and Georgiadis, M. M. (2010) Redox regulation of DNA repair: Implications for human health and cancer therapeutic development. *Antioxid. Redox Signaling* 12, 1247–1269.
- (3) Xanthoudakis, S., and Curran, T. (1992) Identification and characterization of Ref-1, a nuclear protein that facilitates AP-1 DNA-binding activity. *EMBO J.* 11, 653–665.
- (4) Abate, C., Patel, L., Rauscher, F. J. III, and Curran, T. (1990) Redox regulation of fos and jun DNA-binding activity in vitro. *Science* 249, 1157–1161.
- (5) Matthews, J. R., Wakasugi, N., Virelizier, J. L., Yodoi, J., and Hay, R. T. (1992) Thioredoxin regulates the DNA binding activity of NF- κ B by reduction of a disulphide bond involving cysteine 62. *Nucleic Acids Res.* 20, 3821–3830.
- (6) Toledano, M. B., and Leonard, W. J. (1991) Modulation of transcription factor NF- κ B binding activity by oxidation-reduction in vitro. *Proc. Natl. Acad. Sci. U.S.A.* 88, 4328–4332.
- (7) Shimizu, N., Sugimoto, K., Tang, J., Nishi, T., Sato, I., Hiramoto, M., Aizawa, S., Hatakeyama, M., Ohba, R., Hatori, H., Yoshikawa, T., Suzuki, F., Oomori, A., Tanaka, H., Kawaguchi, H., Watanabe, H., and Handa, H. (2000) High-performance affinity beads for identifying drug receptors. *Nat. Biotechnol.* 18, 877–881.
- (8) Ema, M., Hirota, K., Mimura, J., Abe, H., Yodoi, J., Sogawa, K., Poellinger, L., and Fujii-Kuriyama, Y. (1999) Molecular mechanisms of transcription activation by HLF and HIF1 α in response to hypoxia: Their stabilization and redox signal-induced interaction with CBP/p300. *EMBO J.* 18, 1905–1914.
- (9) Ueno, M., Masutani, H., Arai, R. J., Yamauchi, A., Hirota, K., Sakai, T., Inamoto, T., Yamaoka, Y., Yodoi, J., and Nikaido, T. (1999) Thioredoxin-dependent redox regulation of p53-mediated p21 activation. *J. Biol. Chem.* 274, 35809–35815.
- (10) Walker, L. J., Robson, C. N., Black, E., Gillespie, D., and Hickson, I. D. (1993) Identification of residues in the human DNA repair enzyme HAP1 (Ref-1) that are essential for redox regulation of Jun DNA binding. *Mol. Cell. Biol.* 13, 5370–5376.
- (11) Georgiadis, M. M., Luo, M., Gaur, R. K., Delaplane, S., Li, X., and Kelley, M. R. (2008) Evolution of the redox function in mammalian apurinic/apyrimidinic endonuclease. *Mutat. Res.* 643, 54–63.
- (12) Luo, M., Delaplane, S., Jiang, A., Reed, A., He, Y., Fishel, M., Nyland, R. L. II, Borch, R. F., Qiao, X., Georgiadis, M. M., and Kelley, M. R. (2008) Role of the multifunctional DNA repair and redox signaling protein Ape1/Ref-1 in cancer and endothelial cells: Small-molecule inhibition of the redox function of Ape1. *Antioxid. Redox Signaling* 10, 1853–1867.
- (13) Gorman, M. A., Morera, S., Rothwell, D. G., La Fortelle, E., Mol, C. D., Tainer, J. A., Hickson, I. D., and Freemont, P. S. (1997) The

crystal structure of the human DNA repair endonuclease HAP1 suggests the recognition of extra-helical deoxyribose at DNA abasic sites. *EMBO J.* 16, 6548–6558.

(14) Beernink, P. T., Segelke, B. W., Hadi, M. Z., Erzberger, J. P., Wilson, D. M. III, and Rupp, B. (2001) Two divalent metal ions in the active site of a new crystal form of human apurinic/apyrimidinic endonuclease, Ape1: Implications for the catalytic mechanism. *J. Mol. Biol.* 307, 1023–1034.

(15) Mol, C. D., Izumi, T., Mitra, S., and Tainer, J. A. (2000) DNA-bound structures and mutants reveal abasic DNA binding by APE1 and DNA repair coordination [corrected]. *Nature* 403, 451–456.

(16) Kelley, M. R., Luo, M., Reed, A., Su, D., Delaplane, S., Borch, R. F., Nyland, R. L. II, Gross, M. L., and Georgiadis, M. M. (2011) Functional analysis of novel analogues of E3330 that block the redox signaling activity of the multifunctional AP endonuclease/redox signaling enzyme APE1/Ref-1. *Antioxid. Redox Signaling* 14, 1387–1401.

(17) Nyland, R. L., Luo, M., Kelley, M. R., and Borch, R. F. (2010) Design and synthesis of novel quinone inhibitors targeted to the redox function of apurinic/apyrimidinic endonuclease 1/redox enhancing factor-1 (Ape1/ref-1). *J. Med. Chem.* 53, 1200–1210.

(18) Madhusudan, S., Smart, F., Shrimpton, P., Parsons, J. L., Gardiner, L., Houlbrook, S., Talbot, D. C., Hammonds, T., Freemont, P. A., Sternberg, M. J., Dianov, G. L., and Hickson, I. D. (2005) Isolation of a small molecule inhibitor of DNA base excision repair. *Nucleic Acids Res.* 33, 4711–4724.

(19) Bapat, A., Glass, L. S., Luo, M., Fishel, M. L., Long, E. C., Georgiadis, M. M., and Kelley, M. R. (2010) Novel small-molecule inhibitor of apurinic/apyrimidinic endonuclease 1 blocks proliferation and reduces viability of glioblastoma cells. *J. Pharmacol. Exp. Ther.* 334, 988–998.

(20) Jiang, Y., Zhou, S., Sandusky, G. E., Kelley, M. R., and Fishel, M. L. (2010) Reduced expression of DNA repair and redox signaling protein APE1/Ref-1 impairs human pancreatic cancer cell survival, proliferation, and cell cycle progression. *Cancer Invest.* 28, 885–895.

(21) Fishel, M. L., He, Y., Reed, A. M., Chin-Sinex, H., Hutchins, G. D., Mendonca, M. S., and Kelley, M. R. (2008) Knockdown of the DNA repair and redox signaling protein Ape1/Ref-1 blocks ovarian cancer cell and tumor growth. *DNA Repair* 7, 177–186.

(22) Mortensen, P., Gouw, J. W., Olsen, J. V., Ong, S. E., Rigbolt, K. T., Bunkenborg, J., Cox, J., Foster, L. J., Heck, A. J., Blagoev, B., Andersen, J. S., and Mann, M. (2010) MSQuant, an open source platform for mass spectrometry-based quantitative proteomics. *J. Proteome Res.* 9, 393–403.

(23) Xu, H., Zhang, L., and Freitas, M. A. (2008) Identification and characterization of disulfide bonds in proteins and peptides from tandem MS data by use of the MassMatrix MS/MS search engine. *J. Proteome Res.* 7, 138–144.

(24) Xu, H., and Freitas, M. A. (2007) A mass accuracy sensitive probability based scoring algorithm for database searching of tandem mass spectrometry data. *BMC Bioinf.* 8, 133.

(25) Xu, H., Yang, L., and Freitas, M. A. (2008) A robust linear regression based algorithm for automated evaluation of peptide identifications from shotgun proteomics by use of reversed-phase liquid chromatography retention time. *BMC Bioinf.* 9, 347.

(26) Su, D., Delaplane, S., Luo, M., Rempel, D. L., Vu, B., Kelley, M. R., Gross, M. L., and Georgiadis, M. M. (2011) Interactions of Apurinic/Apyrimidinic Endonuclease with a Redox Inhibitor: Evidence for an Alternate Conformation of the Enzyme. *Biochemistry* 50, 82–92.

(27) Walker, L. J., Robson, C. N., Black, E., Gillespie, D., and Hickson, I. D. (1993) Identification of residues in the human DNA repair enzyme HAP1 (Ref-1) that are essential for redox regulation of Jun DNA binding. *Mol. Cell. Biol.* 13, 5370–5376.

(28) Kim, Y.-J., Kim, D., Illuzzi, J. L., Delaplane, S., Su, D., Bemier, M., Gross, M. L., Georgiadis, M. M., and Wilson, D. M. I. (2011) S-Glutathionylation of cysteine 99 in the APE1 protein impairs abasic endonuclease activity. *J. Mol. Biol.* 414, 313–326.

(29) Hirota, K., Matsui, M., Iwata, S., Nishiyama, A., Mori, K., and Yodoi, J. (1997) AP-1 transcriptional activity is regulated by a direct

association between thioredoxin and Ref-1. *Proc. Natl. Acad. Sci. U.S.A.* 94, 3633–3638.

(30) Men, L., Roginskaya, M., Zou, Y., and Wang, Y. (2007) Redox-dependent formation of disulfide bonds in human replication protein A. *Rapid Commun. Mass Spectrom.* 21, 2743–2749.

(31) Day, A. M., and Veal, E. A. (2010) Hydrogen peroxide-sensitive cysteines in the Sty1MAPK regulate the transcriptional response to oxidative stress. *J. Biol. Chem.* 285, 7505–7516.

(32) Chen, C. Y., Willard, D., and Rudolph, J. (2009) Redox regulation of SH2-domain-containing protein tyrosine phosphatases by two backdoor cysteines. *Biochemistry* 48, 1399–1409.

(33) Lametsch, R., Lonergan, S., and Huff-Lonergan, E. (2008) Disulfide bond within μ -calpain active site inhibits activity and autolysis. *Biochim. Biophys. Acta* 1784, 1215–1221.

(34) Holmgren, A. (1995) Thioredoxin structure and mechanism: Conformational changes on oxidation of the active-site sulfhydryls to a disulfide. *Structure* 3, 239–243.